Measurements of the atomistic mechanics of single crystalline silicon wires of nanometer width

Tokushi Kizuka,[1,2,3,*] Yasuhiro Takatani,[1] Koji Asaka,[3] and Ryozo Yoshizaki[1,2]
[1]*Institute of Materials Science, University of Tsukuba, Tsukuba 305-8573, Japan*
[2]*Special Research Project of Nanoscience, University of Tsukuba, Tsukuba 305-8573, Japan*
[3]*Precursory Research for Embryonic Science and Technology, Japan Science and Technology Agency, Tsukuba 305-8573, Japan*
(Received 4 February 2005; revised manuscript received 25 May 2005; published 15 July 2005)

Tensile deformation behavior of silicon (Si) wires with nanometer widths, synthesized by nanometer-tip contact and successive retraction, was studied by atomistic combined microscopy of high-resolution transmission electron microscopy/scanning probe microscopy. The elastic limit, Young's modulus, and strength of individual Si nanowires were investigated based on the mechanics of materials at an atomic scale. It was found that both Young's modulus and strength increased to 18 ± 2 and 5.0 ± 0.3 GPa, respectively. The elastic limit was 0.10 ± 0.02 and fracture strain was estimated to be 0.30 ± 0.01. Experimental results show that mechanical properties of Si wires transform due to size reduction from micrometer to nanometer scale.

DOI: 10.1103/PhysRevB.72.035333 PACS number(s): 73.63.Rt, 68.35.Ja, 68.37.Lp, 68.37.Ps

INTRODUCTION

It has been expected that the mechanical properties of materials will transform as the size of materials is reduced to a nanometer scale with emphases on lattice termination effects at surfaces and restriction in dislocation mechanisms.[1–6] Studies on the mechanical nature of the nanometer-sized structures have been conducted in theoretical simulations for fundamental processes of mechanical interaction at surfaces for adhesion, friction, and nanometer scale machining.[6–14] On the other hand, the experimental research field on this subject was initiated by nanometer scale indentation with scanning electron microscopes[15] and was developed for metallic nanometer-sized contacts with relation to quantized conductance by scanning probe microscopy and by mechanical controllable break junction.[16–26]

In order to study the mechanical properties of nanometer-sized structures, it is required to derive fundamental mechanical constants relating to strength and elasticity from the mechanics of materials on an atomic scale based on measurements of the stress-strain relation for nanometer-sized localized deformation regions. A few experimental works have been attempted for nanometer-sized contacts (nanocontacts) of gold: Stress was evaluated from the estimation of a cross-sectional area of metallic nanocontacts according to the classical Sharvin equation with the Landauer formula.[20–23] In the deformation of monatomic gold wires, stress was estimated using the cross sectional area of single atom.[24,25] It was demonstrated that *in situ* transmission electron microscopy (TEM) had an atomistic spatial resolution for deformation of nanocontacts of metals and isolators.[27–37] In particular, the stress-strain relation for nanometer-sized structures was directly observed by *in situ* TEM combined with sub-nano-Newton force measurement systems.[33,34,37]

Synthesis and electrical properties of silicon (Si) contacts and wires have been extensively studied on nanometer scales.[13,38–58] On the other hand, experiments on the mechanical properties have only been conducted on submicrometer scales.[59–65] In this paper, we demonstrate the mechanics of materials for Si wires of nanometer width, protruding from nanometer Si tips into a vacuum using the *in situ* TEM.

EXPERIMENTAL METHOD

The experimental method in this study was developed based on high-resolution TEM combined with sub-nano-Newton force measurements using atomic force microscopy (AFM) and electronic conductance measurements using scanning tunneling microscopy.[33] A Si cantilever with a nanometer-sized tip, as used in AFM, was attached to the front of a tube piezo on a cantilever holder. The direction of the tip was parallel to the $\langle 100 \rangle$. A Si plate of 0.2 mm thickness was attached to a second sample holder. Both cantilever and plate were prepared from P-doped *n*-type Si with a dopant concentration of $5\times10^{23}/\mathrm{m}^3$ at the surface and a resistivity of $1\sim5\times10^{-4}\ \Omega\,\mathrm{m}$. The thickness of the contact edge of the plate was reduced to 5–20 nm by argon ion milling. The cantilever and the plate holders were then inserted into the combined microscope. The tip of the cantilever was contacted with an edge of the opposing plate by piezo manipulation while applying a bias voltage of 10 V between tip and plate. The tip was pressed into the plate, and then retracted to produce Si wires. A series of these manipulations were performed at room temperature in a vacuum of 1×10^{-5} Pa. The structural dynamics of the process was observed *in situ* by high-resolution TEM using a TV capture system. Thus, the time resolution of the image observations was 17 ms. The force applied between tip and plate were simultaneously measured by optical detection of the cantilever deflection. The electrical conductance was measured using a two-terminal method. The high-resolution imaging and signal detection in this system were simultaneously recorded and analyzed for every image.

RESULTS AND DISCUSSION

Figure 1 shows a time sequence series of high-resolution images of the growth process of a Si nanowire. The tip and the plate before contact are shown in the upper and the lower portions of Fig. 1(a), respectively. The lattice fringes of the

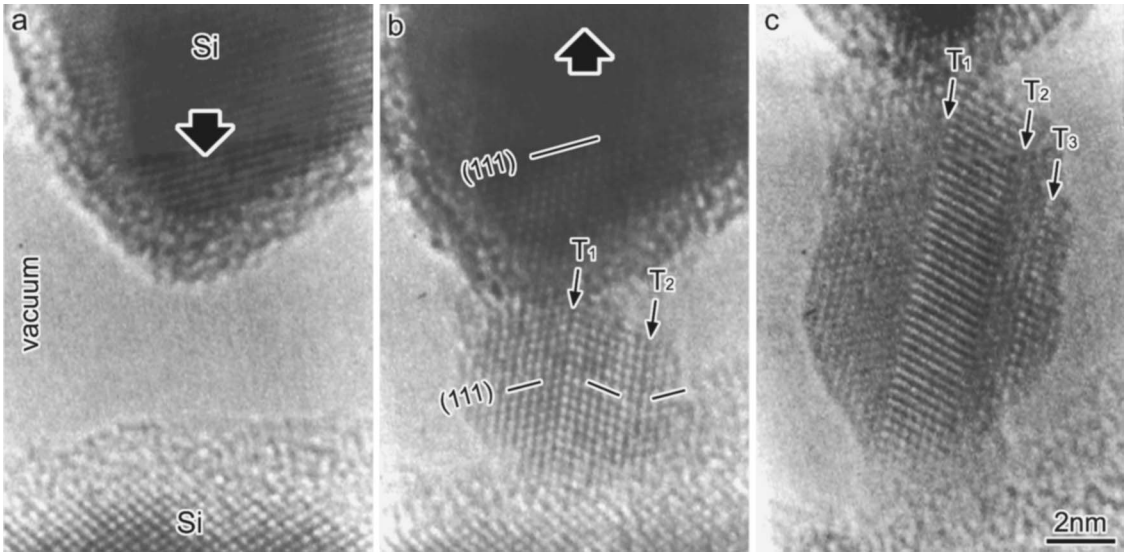

FIG. 1. Time-sequent series of high-resolution images of a nucleation and growth process of a Si nanometer-sized wire. The interval between *a* and *b* is 10 s, and that between *b* and *c* is 11 s. The movement of the tip of the cantilever (upper portion) is indicated by the bold arrows. $T_i(i=1-3)$ designates twin boundaries.

{111} planes of the Si are visible on the tip and the plate. The surfaces of the two crystalline regions are covered with natural oxide layers of 1–2 nm in thickness, which act as insulating layers. After the tip was pressed into the plate, the current increased to more than 100 nA at a bias voltage of 10 V, showing that the insulating layers were broken and the two interior Si crystalline regions were connected. A nucleus forms between the surfaces of the tip and the plate as shown in Fig. 1(b). The nucleus is a Si cluster of approximately 6 nm in diameter. The interval between Figs. 1(a) and 1(b) is 10 s. In this period, the oxide layer is hardly observed on the surfaces of the nucleus as shown in Fig. 1(b). Two {111} faceted twin boundaries are included in the nucleus as indicated by the arrows T_1 and T_2 in Fig. 1(b); the nucleus is constructed of three crystalline regions. The left crystalline region is connected to the tip in a parallel orientation with the tip. The growth rate of the nucleus decreased after contact between tip and plate. The decrease in the rate implies deceleration of atomic diffusion. Current density decreased as contact size increased, thus this nucleation occurs due to current-induced atomic diffusion. The tip was then retracted by piezo manipulation. The one-dimensional crystal growth along the direction of retraction is observed at the contact boundary with the plate as shown in Fig. 1(c), similar to that of the Czochralsky method. A Si wire of 6 nm in width is synthesized between the surfaces of the tip and the plate. The growth occurred intermittently, and as described above, the growth rate was not constant. The two twin boundaries which were induced at the initial nucleation elongate and new one is induced during the growth as indicated by the arrow T_3. Polycrystalline Si wires with nanometer widths formed when twin and general grain boundaries were induced in the nuclei at initial contact or during the growth as shown in Fig. 1. During repetitious contact, nuclei aligned in the same orientation as the tip, i.e., ⟨100⟩, without the formation of any grain boundary, thus nanometer-sized Si wires of single crystalline structures were synthesized. The internal strain energy of the nuclei or wires decreases due to the formation of single crystalline contacts. We used the single crystalline wires as samples for the experiments of the mechanics of materials.

Figure 2 shows a time sequence series of high-resolution images of the tensile deformation process of a single crystalline Si nanowire. The retraction direction in this tensile deformation test is parallel to the ⟨100⟩ as indicated by the bold arrows. In order to estimate elongation and strain, we defined two stationary points as indicated by P_1 on the wire and P_2 on the surface of the plate as shown in Fig. 2(a). The distance between the two points as designated by L_a in Fig. 2(a), L_b in Fig. 2(b), and L_c in Fig. 2(c) elongates due to retraction. In Fig. 2(d), fracture occurs at the contact boundary of the plate surface. Figure 3 shows variations in the strain and the minimal cross sectional area of the wire, force and stress applied to the wire, and current and current density through the wire during the process in Fig. 2 as a function of time. The time associated with the triangles $a-d$ (hereafter the associations *a*, *b*, *c*, and *d*) corresponds to the time in which each image in Figs. 2(a)–2(d) is observed. The strain was estimated from the variation in the distance between P_1 and P_2. The distance of the elongation differs significantly from the movement of the base of the cantilever, i.e., piezo displacement, because entire regions of the tip and the plate are stretched. We assumed that the shape of the cross section of the wire at a minimal width was circular, and estimated the area from the images. We calculated the stress by dividing the force by the minimal cross sectional area. The spatial resolution in this observation is 0.1 nm and gives rise to errors in calculation of the stress and current density. The dimensions of the errors are depicted by the bars in Fig. 3, and are similar to the width of electric noise. The strain increases gradually between 0 s to time *a*, and between time *b* and time *c* in Fig. 3. The force increases from 0 s to the time *a*, and then is abruptly reduced. It is seen from the high-resolution images in Figs. 2(a) and 2(b) that the wire elongates and the width

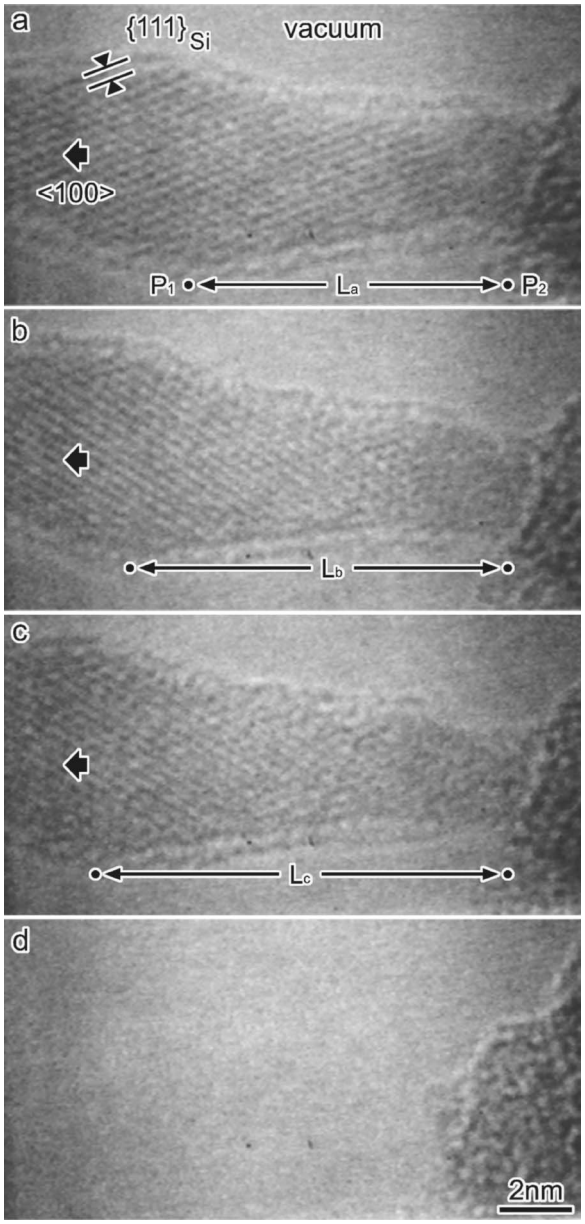

FIG. 2. Time-sequent series of high-resolution images of a tensile deformation process of a single crystalline Si nanowire. The tip of the cantilever (the left-hand side) is retracted towards the left as indicated by the bold arrows.

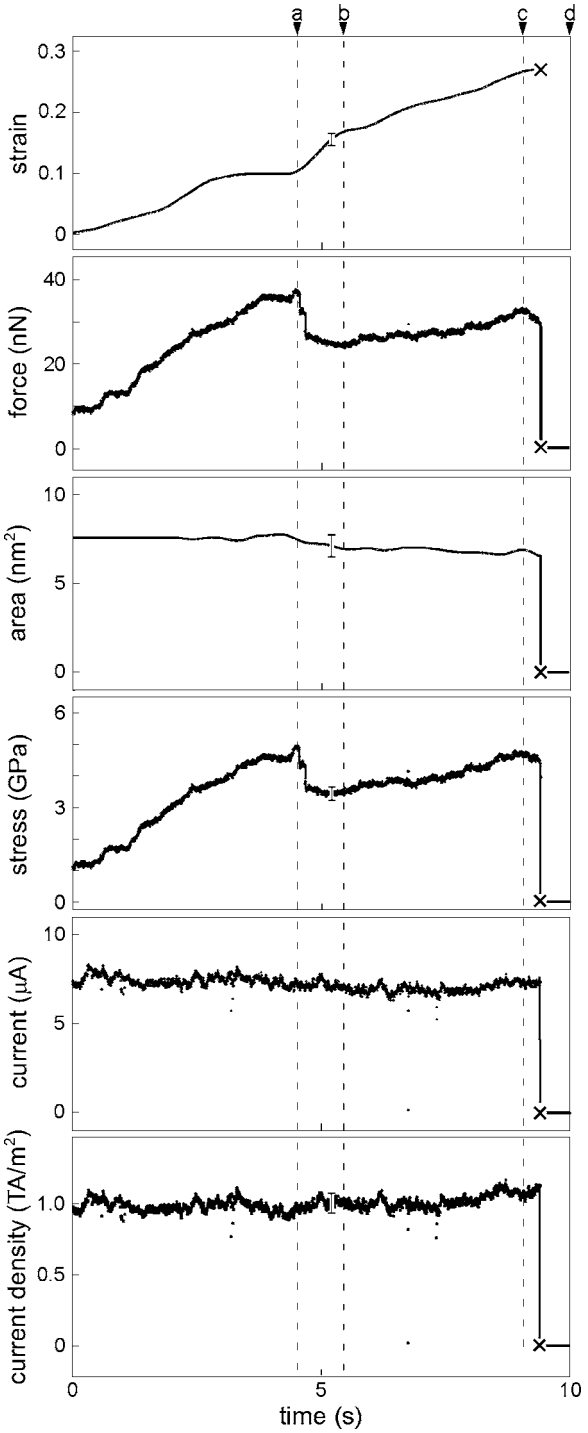

FIG. 3. Variations in strain, force, minimal cross sectional area, stress, current, and current density during the tensile deformation process in Fig. 2 as a function of time. The time with the triangles *a–d* corresponds to the time at the recording of the images of *a–d* in Fig. 2. The cross indicates fracture.

decreases in the right-hand side of the wire near the contact boundary. The process of the elongation and the decrease in the width were different from the elastic deformation process from 0 s to time *a*. The rapid decrease in force and this structural change imply that plastic deformation occurs between time *a* and time *b*. The strain and force then increase gradually from time *b* to time *c* again as that from 0 s to time *a*, whereas the minimal cross sectional area reduces. The force and stress then begin to decrease slightly from time *c* to the fracture. The decrease in force and stress from time *c* onward shows that structural relaxation takes place as precursor phenomena of the fracture. Therefore, the wire deforms elastically from time *b* to time *c* and two typical elastic regions are found in the periods from 0 s to time $a(\Delta T_{E1})$ and in time b to $c(\Delta T_{E2})$.

In order to develop analyses based on mechanics of materials for the wire, we derived the stress-strain relation as shown in Fig. 4 for the tensile deformation observed in Fig. 3. Tensile strength for the nanowire, i.e., the maximum

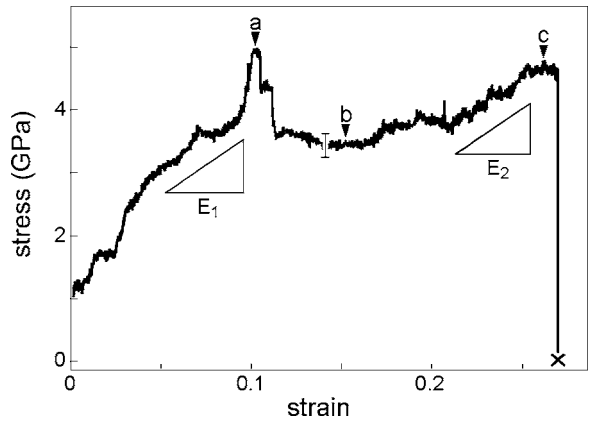

FIG. 4. Stress-strain curve in the tensile deformation process in Fig. 2. The cross indicates fracture.

stress, is 5.0±0.3 GPa at times *a* and *c*. The relation for two elastic regions is not linear, and we selected relatively straight slope regions for the estimation of Young's modulus as indicated with E_1 and E_2 in Fig. 4, corresponding to the periods ΔT_{E1} and ΔT_{E2}, Young's modulus estimated from the two regions is 18±2 GPa. Elastic limits for the initial elastic region E_1, corresponding to the dimension of the region, is 0.10±0.02. Fracture occurs at a strain of 0.27±0.01. This strain is not equal to maximum elastic limit, because the plastic deformation occurs at time *a*. Extrapolating from the rate between the Young's modulus and strength, the maximum elastic limit up to fracture is calculated to be 0.30±0.01. Thus, due to the plastic deformation around time *a*, strain is reduced by 0.03.

The Young's modulus for the ⟨100⟩ of millimeter-sized pure and doped Si with dislocation density of less than $500/\mathrm{cm}^2$ is ~170 GPa.[59] The calculated modulus for the ⟨100⟩ by Brantley is 1.3×10^2 GPa.[60] For micrometer-sized Si samples of 20–30 μm in thickness, 100 μm in width and 400 μm in length, fracture strain and Young's modulus along the ⟨100⟩ direction are 0.015 and 140 GPa.[61] This Young's modulus is also similar to the calculated values according to Brantley[60] and the strength of the micrometer-sized samples is estimated to be 2.1 GPa.[62] Another important direction for the deformation is the ⟨110⟩. For the ⟨110⟩ direction, Si wires of 50–300 μm in width and 6 mm in length, Young's modulus, and the strength are 142–169 GPa and 1–2 GPa, respectively,[62] which is similar to the calculated values.[60] For thinner samples of 0.14 μm in thickness, 20 μm in width and 100 μm in length, Young's modulus was estimated to be 169 GPa.[63] For the ⟨100⟩ and ⟨110⟩ directions, these previous results involving the Young's modulus is hardly influenced by the size reduction from millimeter to micrometer scale. On the other hand, for the ⟨110⟩ direction, the strength for the thinner samples of 0.14 μm in thickness increased to 4.9 GPa at the fracture strain of 0.031.[63]

In this experiment, the strength of the single crystalline nanowire increases to twice of that of the micrometer-sized samples.[61] The strength of crystals is determined by defect generation and evolution.[4,5] In particular in Si, pre-existing defects act as origins for cracks. The strength is determined at the fracture by crack evolution.[4,5] Inside the single crystalline nanowires in this experiment, no dislocation could be observed and fractures occurred in the weakest regions, i.e., the regions having minimal widths. The strength observed in this nanowire shows the strength of dislocation-free nanometer scale Si. For nanometer-sized metallic contacts, the strength is 10–50 times larger than that of bulk.[21,23,24,33] This difference is attributed to the behavior of dislocations in metals.[3,4,5] The dislocations exist in metals even when the size is reduced to a few tenths of nanometers.[65]

The elastic limit of the nanowire is approximately 6 times larger that of the micrometer-sized samples.[61] The average value of the Young's modulus is approximately 0.1–0.13 of that of the micrometer-sized samples.[61] Elastic properties are dependent on the nature of bonding of materials. In this experiment, the size of the structures was reduced to less than 10 nm. This shows that elastic properties, which are determined by the bonding nature, transforms due to the size reduction of the nanometer scale.

In Fig. 3, the variation in current resembles that of the minimal cross sectional area, showing the current is determined by the constriction. The current density is approximately 1×10^{12} A/m^2. This current density is similar to the contacts of ~5 nm^2 in area between clean Si {111} surfaces and tungsten tips,[67] and is 10^4–10^5 times larger than that of the Si wires of more than few tenths of nanometers in width.[49,57,58] The cross sectional area for one atomic column along the ⟨100⟩ in bulk Si is 0.037 nm^2. Adopting this area, current through the one atomic column of the nanowire in this experiment is estimated from the current density in Fig. 3 to be 37 nA. This current is 50–100 times larger than tunneling current.[66,67]

CONCLUSION

We have performed the experiment on the mechanics of materials in the atomic scale for the single crystalline Si nanowires using the atomistic combined microscope. From the measurement of stress-strain relations, the transformation of the mechanical properties by the size reduction to nanometer scale was elucidated. In particular, the increase in the elastic limit to 0.10±0.02 and in the fracture strain to 0.30±0.01 shows that the bonding nature of nanometer-sized Si wires differs from that of the micrometer-sized Si wires.

ACKNOWLEDGMENTS

The authors would like to thank Dr. S. Fujisawa and Dr. A. Yabe of the National Institute of Advanced Industrial Science and Technology for cooperation in developing the nano-Newton force measurement system. This work was partly supported by the funds for the Special Research Project on Nanoscience and the University Research Projects of the University of Tsukuba. Financial support was provided by the Nippon Sheet Glass Foundation and by a Grant-In-Aid from the Ministry of Education, Science, Sport and Culture (Grant Nos. 14350018, 16656040).

*Email address: kizuka@ims.tsukuba.ac.jp

[1] M. R. Hoare and P. Pal, J. Cryst. Growth **17**, 771 (1972).
[2] P. M. Ajayan and L. D. Marks, Phys. Rev. Lett. **60**, 585 (1988).
[3] J. Weertman and J. R. Weertman, *Elementary Dislocation Theory* (Oxford University Press, Oxford, 1992).
[4] B. Lawn, *Fracture in Brittle Solids* (Cambridge University Press, Cambridge, 1975).
[5] L. B. Freund and S. Suresh, *Thin Film Materials, Stress, Defect Formation and Surface Evolution* (Cambridge University Press, Cambridge, 2003).
[6] U. Landman, W. D. Luedtke, N. A. Burnham, and R. J. Colton, Science **248**, 454 (1990).
[7] S. Ciraci, E. Tekman, M. Gökçedag, I. P. Batra, and A. Baratoff, Ultramicroscopy **42**, 163 (1992).
[8] T. N. Todorov and A. P. Sutton, Phys. Rev. Lett. **70**, 2138 (1993).
[9] R. M. Lynden-Bell, Science **263**, 1704 (1994).
[10] J. A. Torres and J. J. Sáenz, Phys. Rev. Lett. **77**, 2245 (1996).
[11] R. N. Barnett and U. Landman, Nature (London) **387**, 788 (1997).
[12] M. R. Sorensen, M. Brandbyge, and K. W. Jacobsen, Phys. Rev. B **57**, 3283 (1998).
[13] U. Landman, R. N. Barnett, A. G. Scherbakov, and P. Avouris, Phys. Rev. Lett. **85**, 1958 (2000).
[14] S. R. Bahn and K. W. Jacobsen, Phys. Rev. Lett. **87**, 266101 (2001).
[15] M. D. Pashley and J. B. Pethica, J. Vac. Sci. Technol. A **3**, 757 (1985).
[16] *Nanowires*, edited by P. A. Serena and N. Garcia, Vol. 340 of *NATO Advanced Studies Institute, Series E: Applied Sciences* (Kluwer, Dordrecht, 1997).
[17] U. Dürig, O. Züger, and D. W. Pohl, Phys. Rev. Lett. **65**, 349 (1990).
[18] J. K. Gimzewski and R. Möller, Phys. Rev. B **36**, R1284 (1987).
[19] N. A. Burnham, R. J. Colton, and H. M. Pollock, Nanotechnology **4**, 64 (1993).
[20] N. Agraït, J. G. Rodrigo, G. Rubio, C. Sirvent, and S. Vieira, Thin Solid Films **253**, 199 (1994).
[21] U. Dürig, O. Züger, and A. Stalder, J. Appl. Phys. **72**, 1778 (1992).
[22] G. Rubio, N. Agraït, and S. Vieira, Phys. Rev. Lett. **74**, 3995 (1995).
[23] G. Rubio, N. Agraït, and S. Vieira, Phys. Rev. Lett. **76**, 2302 (1996).
[24] G. Rubio-Bollinger, S. R. Bahn, N. Agraït, K. W. Jacobsen, and S. Vieira, Phys. Rev. Lett. **87**, 026101 (2001).
[25] J. M. Krans, J. M. van Ruitenbeek, V. V. Fisum, I. K. Yanson, and L. J. de Jongh, Nature (London) **375**, 767 (1995).
[26] A. Stalder and U. Dürig, J. Vac. Sci. Technol. B **14**, 1259 (1996).
[27] M. I. Lutwyche and Y. Wada, Appl. Phys. Lett. **66**, 2807 (1994).
[28] T. Kizuka, K. Yamada, S. Deguchi, M. Naruse, and N. Tanaka, Phys. Rev. B **55**, R7398 (1997).
[29] T. Kizuka, Phys. Rev. Lett. **81**, 4448 (1998).
[30] H. Ohnishi, Y. Kondo, and K. Takayanagi, Nature (London) **395**, 780 (1998).
[31] V. Rodrigues, T. Fuhrer, and D. Ugarte, Phys. Rev. Lett. **85**, 4124 (2000).
[32] T. Kizuka, S. Umehara, and S. Fujisawa, Jpn. J. Appl. Phys., Part 2 **40**, L71 (2001).
[33] T. Kizuka, H. Ohmi, T. Sumi, K. Kumazawa, S. Deguchi, M. Naruse, S. Fujisawa, S. Sasaki, A. Yabe, and Y. Enomoto, Jpn. J. Appl. Phys., Part 2 **40**, L170 (2001).
[34] D. Erts, A. Lõhmus, R. Lõhmus, and H. Olin, Appl. Phys. A: Mater. Sci. Process. **72**, S71 (2001).
[35] Y. Takai, T. Kawasaki, Y. Kimura, T. Ikuta, and R. Shimizu, Phys. Rev. Lett. **87**, 106105 (2001).
[36] S. B. Legoas, D. S. Galvão, V. Rodrigues, and D. Ugarte, Phys. Rev. Lett. **88**, 076105 (2002).
[37] D. Erts, A. Lõhmus, R. Lõhmus, H. Olin, A. V. Pokropivny, L. Ryen, and K. Svensson, Appl. Surf. Sci. **188**, 460 (2002).
[38] A. G. Cullis and L. T. Canham, Nature (London) **353**, 335 (1991).
[39] A. J. Read, R. J. Needs, K. J. Nash, L. T. Canham, P. D. J. Calcott, and A. Qteish, Phys. Rev. Lett. **69**, 1232 (1992).
[40] A. G. Nassiopoulos, S. Grigoropoulos, and D. Papadimitriou, Appl. Phys. Lett. **69**, 2267 (1996).
[41] T. Makimura, Y. Kunii, and K. Murakami, Jpn. J. Appl. Phys., Part 1 **35**, 4780 (1996).
[42] Z. A. K. Durrani, T. Kamiya, Y. T. Tan, H. Ahmed, and N. Lloyd, Microelectron. Eng. **63**, 267 (2002).
[43] J. Westwater, D. P. Gosain, S. Tomiya, S. Usui, and H. Ruda, J. Vac. Sci. Technol. B **15**, 554 (1997).
[44] A. M. Morales and C. M. Lieber, Science **279**, 208 (1998).
[45] N. Ozaki, Y. Ohno, and S. Takeda, Appl. Phys. Lett. **73**, 3700 (1998).
[46] D. D. D. Ma, C. S. Lee, F. C. K. Au, S. Y. Tong, and S. T. Lee, Science **299**, 1874 (2003).
[47] Y. F. Zhang, Y. H. Tang, N. Wang, D. P. Yu, C. S. Lee, I. Bello, and S. T. Lee, Appl. Phys. Lett. **72**, 1835 (1998).
[48] G. F. Grom, D. J. Lockwood, J. P. McCaffrey, H. J. Labbé, P. M. Fauchet, B. White, Jr., J. Diener, D. Kovalev, F. Koch, and L. Tsybeskov, Nature (London) **407**, 358 (2000).
[49] Y. Nakajima, Y. Takahashi, S. Horiguchi, K. Iwadate, H. Namatsu, K. Kurihara, and M. Tabe, Appl. Phys. Lett. **65**, 2833 (1994).
[50] H. Ishikuro, T. Fujii, T. Saraya, G. Hashiguchi, T. Hiramoto, and T. Ikoma, Appl. Phys. Lett. **68**, 3585 (1996).
[51] N. Clément, D. Tonneau, H. Dallaporta, V. Bouchiat, D. Fraboulet, D. Mariole, J. Gautier, and V. Safarov, Physica E (Amsterdam) **13**, 999 (2002).
[52] R. Hasunuma, T. Komeda, H. Mukaida, and H. Tokumoto, J. Vac. Sci. Technol. B **15**, 1437 (1997).
[53] S. Heike, T. Hashizume, and Y. Wada, J. Appl. Phys. **80**, 4182 (1996).
[54] T. Ono, H. Saitoh, and M. Esashi, Appl. Phys. Lett. **70**, 1852 (1997).
[55] Y. Naitoh, K. Takayanagi, Y. Oshima, and H. Hirayama, J. Electron Microsc. **49**, 211 (2000).
[56] T. Kizuka, Phys. Rev. B **63**, 033309 (2001).
[57] S. F. Hu, W. Z. Wong, S. S. Liu, Y. C. Wu, C. L. Sung, and T. Y. Hung, Solid State Commun. **125**, 351 (2003).
[58] S. Chung, J. Yu, and J. R. Heath, Appl. Phys. Lett. **76**, 2068 (2000).
[59] J. J. Hall, Phys. Rev. **161**, 756 (1967).
[60] W. A. Brantley, J. Appl. Phys. **44**, 534 (1973).
[61] K. Sato, T. Yoshioka, T. Ando, M. Shikida, and T. Kawabata, Sens. Actuators, A **70**, 106 (1998).
[62] T. Yi, L. Li, and C. J. Kim, Sens. Actuators, A **83**, 172 (2000).
[63] T. Tsuchiya, M. Shikida, and K. Sato, Sens. Actuators, A **97-98**,

492 (2002).
[64] J. A. Hauch, D. Holland, M. P. Marder, and H. L. Swinney, Phys. Rev. Lett. **82**, 3823 (1999).
[65] T. Kizuka, Phys. Rev. B **57**, 11 158 (1998).
[66] R. Hasunuma, T. Komeda, and H. Tokumoto, Appl. Surf. Sci. **130-132**, 84 (1998).
[67] R. Hasunuma, T. Komeda, and H. Tokumoto, Jpn. J. Appl. Phys., Part 1 **36**, 3827 (1997).